



# Measurements of a potential interference with laser-induced fluorescence measurements of ambient OH from the ozonolysis of biogenic alkenes

Pamela Rickly<sup>1</sup> and Philip S. Stevens<sup>1,2</sup>

<sup>1</sup>School of Public and Environmental Affairs, Indiana University, Bloomington, IN, USA

<sup>2</sup>Department of Chemistry, Indiana University, Bloomington, IN, USA

**Correspondence:** Philip S. Stevens (pstevens@indiana.edu)

Received: 16 June 2017 – Discussion started: 21 June 2017

Revised: 10 November 2017 – Accepted: 16 November 2017 – Published: 3 January 2018

**Abstract.** Reactions of the hydroxyl radical (OH) play a central role in the chemistry of the atmosphere, and measurements of its concentration can provide a rigorous test of our understanding of atmospheric oxidation. Several recent studies have shown large discrepancies between measured and modeled OH concentrations in forested areas impacted by emissions of biogenic volatile organic compounds (BVOCs), where modeled concentrations were significantly lower than measurements. A potential reason for some of these discrepancies involves interferences associated with the measurement of OH using the laser-induced fluorescence–fluorescence assay by gas expansion (LIF-FAGE) technique in these environments. In this study, a turbulent flow reactor operating at atmospheric pressure was coupled to a LIF-FAGE cell and the OH signal produced from the ozonolysis of  $\alpha$ -pinene,  $\beta$ -pinene, ocimene, isoprene, and 2-methyl-3-buten-2-ol (MBO) was measured. To distinguish between OH produced from the ozonolysis reactions and any OH artifact produced inside the LIF-FAGE cell, an external chemical scrubbing technique was used, allowing for the direct measurement of any interference. An interference under high ozone (between  $2 \times 10^{13}$  and  $10 \times 10^{13}$  cm<sup>-3</sup>) and BVOC concentrations (between approximately  $0.1 \times 10^{12}$  and  $40 \times 10^{12}$  cm<sup>-3</sup>) was observed that was not laser generated and was independent of the ozonolysis reaction time. For the ozonolysis of  $\alpha$ - and  $\beta$ -pinene, the observed interference accounted for approximately 40 % of the total OH signal, while for the ozonolysis of ocimene the observed interference accounted for approximately 70 % of the total OH signal. Addition of acetic acid to the reactor eliminated the interference, suggesting that the source of the interference in

these experiments involved the decomposition of stabilized Criegee intermediates (SCIs) inside the FAGE detection cell. Extrapolation of these measurements to ambient concentrations suggests that these interferences should be below the detection limit of the instrument.

## 1 Introduction

The hydroxyl radical (OH) plays an important role in the chemistry of the atmosphere. OH initiates the oxidation of volatile organic compounds (VOCs) which in the presence of nitrogen oxides (NO<sub>x</sub>) can lead to the production of ozone and secondary organic aerosols, the primary components of photochemical smog. Because of its high reactivity, measurements of OH can provide a rigorous test of our understanding of the fast radical chemistry in the atmosphere. However, several field campaigns have identified significant discrepancies between measured and modeled OH concentrations, especially in low-NO<sub>x</sub> forested environments (Rohrer et al., 2014). For example, Ren et al. (2008) found that OH concentrations were well predicted by models to within their combined estimated uncertainty when mixing ratios of isoprene were less than approximately 500 pptv, but measurements acquired in areas with higher mixing ratios of isoprene showed observed OH concentrations that were 3–5 times larger than model predictions. Similarly, measurements in a northern Michigan forest found daytime OH concentrations approximately 3 times larger and nighttime concentrations 3–10 times larger than model predictions (Tan et al., 2001; Faloona et al., 2001). Aircraft measurements over the Ama-

zon rainforest found OH concentrations to be 40–80 % larger than model predictions (Lelieveld et al., 2008), while measurements of OH in the Borneo rainforest were 5–10 times greater than model predictions (Whalley et al., 2011). Similarly, measurements of OH concentrations under high mixing ratios of isoprene in the Pearl River Delta, China, were 3–5 times larger than model predictions (Hofzumahaus et al., 2009).

Most of these measurements were done using the laser-induced fluorescence–fluorescence assay by gas expansion (LIF-FAGE) technique. In this technique, ambient air is sampled through an inlet at low pressure, enhancing the OH fluorescence lifetime and allowing temporal filtering of the OH fluorescence from laser scatter (Heard and Pilling, 2003). Fluorescence from OH radicals is distinguished from background scatter and broadband fluorescence through spectral modulation of the laser wavelength. Previous laboratory tests using the Penn State instrument demonstrated that the technique was free from interferences from several species, including spectral interferences from naphthalene, sulfur dioxide, and formaldehyde, as well as chemical interferences from high concentrations of H<sub>2</sub>O<sub>2</sub>, HONO, SO<sub>2</sub>, HNO<sub>3</sub>, several alcohols and alkanes, propene, and isoprene (Ren et al., 2004). Mixtures of ozone with ethene, propylene, and isoprene did not result in any significant signal, suggesting that the ozonolysis of these compounds did not produce an interference in the Penn State instrument, although small interferences were observed with addition of high amounts of ozone and acetone that would be insignificant under ambient conditions (Ren et al., 2004). Measurements of OH in the SAPHIR chamber at atmospheric pressure and under varying concentrations of H<sub>2</sub>O, O<sub>3</sub>, CO, HCHO, NO, and NO<sub>2</sub> by both an LIF-FAGE instrument and a differential optical absorption spectroscopy (DOAS) instrument were in excellent agreement, suggesting that measurements of OH using the LIF-FAGE instrument were free from artifacts under these conditions (Schlossler et al., 2007). A subsequent intercomparison inside the SAPHIR chamber found that measurements from several different LIF-FAGE instruments under a variety of conditions agreed with each other to within the calibration accuracies of the instruments (Schlossler et al., 2009). No interferences were detected under varying concentrations of O<sub>3</sub>, H<sub>2</sub>O, NO<sub>x</sub> and peroxy radicals, and measurements of OH during the ozonolysis of various mixing ratios of pent-1-ene (6–25 ppb) and trans-2-butene (200 ppb) in approximately 100 ppb of ozone also did not reveal a significant interference (Schlossler et al., 2009). In contrast, Hard et al. (2002) observed an interference in their LIF-FAGE instrument during calibrations using the ozonolysis of trans-2-butene under high mixing ratios of both ozone and trans-2-butene. Tests suggested that the interference was not laser generated and disappeared in air containing 1 % water vapor. They suggested that the interference may be due to the dissociation of an intermediate in the ozonolysis mechanism that

produces OH in the low-pressure cell of their FAGE instrument (Hard et al., 2002).

Recently, Mao et al. (2012) discovered a significant interference associated with their LIF-FAGE measurements of OH in a northern California forest. Using a chemical scavenger to remove ambient OH before air enters the inlet, they found that subsequent spectral modulation revealed a significant amount of internally generated OH from an unknown interference. Measurements using only spectral modulation of the laser wavelength were greater than the measurements when the interference measured using the chemical scavenger was subtracted, and the latter measurements were in better agreement with model predictions (Mao et al., 2012). Similar results were observed by Novelli et al. (2014a), who measured ambient OH concentrations in several forest environments using an external chemical scavenger technique. They found that OH generated inside their detection cell comprised 30–80 % of the daytime signal observed using spectral modulation and 60–100 % of the signal observed at night. Subtracting the interference from the ambient signal resulted in OH concentrations that were in good agreement with model simulations as well as measurements by a chemical ionization mass spectrometry (CIMS) instrument (Novelli et al., 2014a).

Mao et al. (2012) found that the interference increased with both temperature and measured OH reactivity, suggesting that the interference was related to biogenic emissions in this environment, perhaps the result of biogenic volatile organic compound (BVOC) oxidation products entering the sampling cell of the LIF-FAGE instrument which subsequently undergo further reactions and/or decomposition producing the additional OH signal. Novelli et al. (2017) also found that the interference appeared to correlate with temperature similar to the temperature dependence of terpene emissions and was also correlated with the measured ozone concentrations. They concluded that one possible contributor to their interference was the decomposition of stabilized Criegee intermediates (SCIs) inside their instrument. In addition to decomposition leading to OH formation at ambient pressure (Fang et al., 2016; Kidwell et al., 2016; Smith et al., 2016), previous laboratory experiments have shown that BVOC ozonolysis intermediates, such as Criegee intermediates and vinyl hydroperoxides, are likely to promptly decompose to produce OH at low pressures (Kroll et al., 2001a, b). As a result of the large pressure and temperature gradients which occur as the sample enters the FAGE detection cell, the dissociation pathway of these intermediate species may be favored, leading to additional OH production. Recently, Fuchs et al. (2016) performed laboratory and chamber experiments to determine whether the ozonolysis of alkenes produced an OH artifact in their LIF-FAGE instrument. They found that, under reactant concentrations that were orders of magnitude greater than ambient, the ozonolysis of propene,  $\alpha$ -pinene, limonene, and isoprene produced a detectable interference in their instrument that increased with

the turnover rate of the reaction. Extrapolating their results to ambient concentrations of ozone and alkenes would suggest that the ozonolysis of these compounds would not produce a detectable interference in their instrument under ambient conditions (Fuchs et al., 2016).

The goal of this work is to determine whether intermediates or products in the ozonolysis of various biogenic alkenes can lead to an interference with OH measurements using the Indiana University LIF-FAGE instrument (IU-FAGE). These experiments focus on the ozonolysis of several biogenic alkenes, including  $\alpha$ -pinene,  $\beta$ -pinene, ocimene, isoprene, and 2-methyl-3-buten-2-ol (MBO), all of which have been observed to contribute appreciably to BVOC emissions in forested environments (Guenther et al., 1994; Harley et al., 1998). Measurements of the interference as a function of various instrumental parameters are also provided in an attempt to identify possible sources of the interference and ways it could be minimized.

## 2 Experimental section

The ozonolysis experiments were performed using an atmospheric pressure turbulent flow tube with a movable injector similar to that used for ambient measurements of total OH reactivity (Hansen et al., 2014). The 1 m long and 5 cm diameter flow tube was positioned perpendicular to the IU-FAGE detection cell so that the flow would not interfere with the external OH scavenging measurement (Sect. 2.2; Fig. 1). A Teflon adaptor attached at one end of the flow tube supported the injector, a 1 m stainless steel tube with a 1.25 cm diameter. This injector allowed for the introduction of ozone produced from an ozone generator (Enaly) to the system and could be moved throughout the flow tube to permit varying reaction times between approximately 100 and 420 ms calculated based on the measured velocity in the flow tube. Attached to the end of the injector was a turbulizer used to increase mixing of the reagents at the start of the reaction. A flow of nitrogen of 180 SLPM created a turbulent flow with a Reynolds number of approximately 3750. Ozone concentrations were varied between approximately 1 and 3 ppm ( $2 \times 10^{13}$ – $7 \times 10^{13}$  molecules  $\text{cm}^{-3}$ ), with most measurements occurring at ozone concentrations of 2.5, 5, and  $7 \times 10^{13}$  molecules  $\text{cm}^{-3}$  as the ozone generator provided the highest stability at these concentrations. Ozone concentrations in the flow tube were measured using a Teledyne photometric ozone analyzer (model 400E), with an estimated uncertainty of  $\pm 0.5$  ppb.

BVOC concentrations were introduced into the flow tube by bubbling  $\text{N}_2$  through the liquid compound sending the vapor into the reactor. The concentration of the BVOC was estimated from its equilibrium vapor pressure and accounting for dilution into the main flow. Several alkene concentrations were used for each experiment, with approximate concentrations of  $2 \times 10^{11}$  to  $4 \times 10^{13}$  molecules  $\text{cm}^{-3}$  for  $\alpha$ -pinene

(Aldrich, 98 %),  $1 \times 10^{11}$  to  $4 \times 10^{13}$  molecules  $\text{cm}^{-3}$  for  $\beta$ -pinene (Aldrich, 99 %),  $9 \times 10^{10}$  to  $5 \times 10^{13}$  molecules  $\text{cm}^{-3}$  for ocimene (Aldrich, mixture of isomers, >90 %), and approximately  $8 \times 10^{13}$  molecules  $\text{cm}^{-3}$  for isoprene (Aldrich, 99 %), and MBO (Aldrich, 98 %). Unfortunately, no direct method for measuring the concentration of these BVOCs was available, and as a result the absolute concentration of BVOCs in the flow tube is highly uncertain due to potential wall losses prior to entering the flow tube.

### 2.1 Detection of OH radicals

OH radicals were measured using the IU-FAGE instrument, in which ambient air is pulled through either a 0.6 or 1 mm diameter nozzle and expanded to a total pressure of approximately 4–9 Torr resulting in a total flow rate of approximately 3–10 SLPM (Dusanter et al., 2008, 2009; Griffith et al., 2013, 2016). Previous field measurements using the IU-FAGE instrument have incorporated a cylindrical inlet (5 cm diameter, 14 cm long) attached to the main detection block resulting in a total distance of approximately 20 cm from the nozzle to the detection volume (Fig. 2). These previous field measurements have utilized both the 0.6 mm nozzle (Griffith et al., 2016) and the 1 mm nozzle (Dusanter et al., 2009; Griffith et al., 2013), and the experiments presented here have attempted to reproduce these instrument configurations.

The original IU-FAGE laser system used in this study consisted of a Spectra-Physics Navigator II YHP40-532Q diode-pumped Nd:YAG laser that produces approximately 5.5 W of radiation at 532 nm at a repetition rate of 5 kHz. This laser pumped a Lambda Physik Scanmate 1 dye laser (Rhodamine 640, 0.25 g  $\text{L}^{-1}$  in isopropanol) that produced tunable radiation around 616 nm, which was frequency doubled to generate 2 to 20 mW of radiation at 308 nm. This laser system was recently replaced with a Spectra-Physics Navigator II YHP40-532Q that produces approximately 8 W of radiation at 532 nm at a repetition rate of 10 kHz that pumps a Sirah Credo dye laser (255 mg  $\text{L}^{-1}$  of Rhodamine 610 and 80 mg  $\text{L}^{-1}$  of Rhodamine 101 in ethanol), resulting in 40 to 100 mW of radiation at 308 nm. Initial measurements of the OH interference from ocimene and  $\alpha$ -pinene ozonolysis were made using the original laser system, with the majority of experiments done using the newer laser system.

After exiting the dye laser, the beam is focused onto a 12 m optical fiber to transmit the radiation to the sampling cell where it crosses the expanded air perpendicular to the flow approximately 24 times in a multipass White cell configuration (Fig. 2). The OH molecule is excited and detected using the  $A^2\Sigma^+ (v' = 0) \leftarrow X^2\Pi_i (v'' = 0)$  transition near 308 nm. A reference cell where OH is produced by thermal dissociation of water vapor is used to ensure that the laser is correctly tuned on and off of the OH transition to measure the net fluorescence signal. The OH fluorescence is detected by a gated microchannel plate detector (Hamamatsu R5916U-52) and the resulting signal is sent through a preamplifier (Stan-

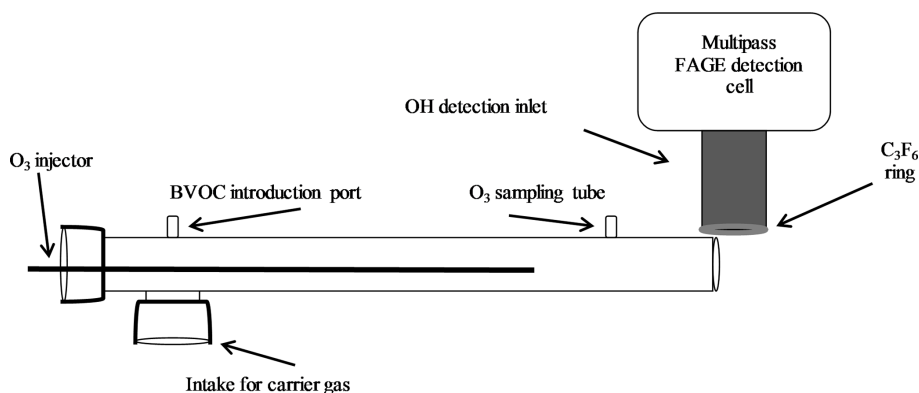


**Figure 1.** Schematic of the atmospheric pressure flow system used in this study.

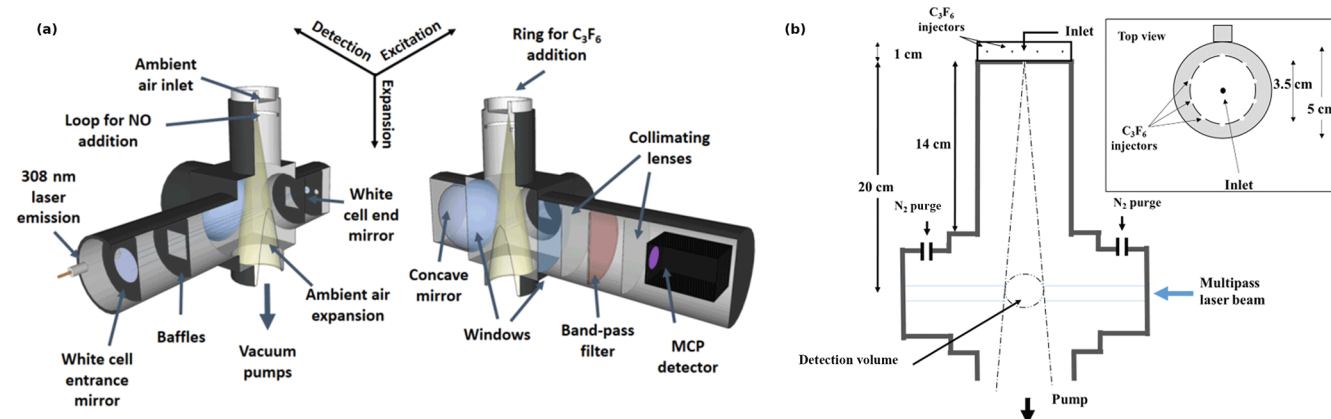


**Figure 2.** Schematic of the IU-FAGE sampling and excitation axis (a) and cross section with dimensions for the medium inlet configuration (b).

ford Research Systems SR445) and a photon counter (Stanford Research Systems SR400). The detector is switched off during the laser pulse through the use of electronic gating, allowing the OH fluorescence to be temporally filtered from laser scatter. Each offline measurement is recorded for approximately 10 s and is averaged and subtracted from the online measurement, averaged for approximately 20 s. These measurements are recorded for at least 5 cycles per ozone concentration once the OH concentration has stabilized after several minutes.

The sensitivity of the IU-FAGE instrument was calibrated using the UV-water photolysis technique where water vapor is photolyzed to produce known amounts of OH (Dusanter et al., 2008). In these experiments, calibrations were performed under the conditions of the experiments using  $N_2$ , resulting in larger calibration factors compared to ambient air due to fluorescence quenching by oxygen. Nitrogen from liquid boil-off was used instead of synthetic air to reduce the concentration of reactive impurities in the flow tube. The  $N_2$  calibration factors were determined for various instrumental parameters including three cell pressures (4, 7, and 9 Torr), the two nozzle diameters (0.6 and 1 mm), and three inlet lengths (3.2, 14,

and 24.8 cm; Table S1, Fig. S1 in the Supplement). For reference, previous ambient measurements using the IU-FAGE instrument were typically acquired using the medium inlet length (Fig. 2) and both the 0.6 and 1 mm nozzle diameters, resulting in cell pressures of 4–7 Torr depending on the nozzle diameter size and pumping efficiency (Lew et al., 2017a). The error associated with the UV-water photolysis calibration technique is estimated to be  $\pm 36\%$  ( $2\sigma$ ; Dusanter et al., 2008).

Both nozzle diameters showed similar sensitivities that decreased as the pressure increased due to increased collisional quenching of the OH fluorescence. The calibration factor was also sensitive to the length of the inlet where the ambient air enters the cell and where the OH fluorescence occurs in the detection axis, with the sensitivity decreasing with the increasing inlet length likely due to increased loss of OH radicals on the interior walls of the inlet. For these experiments, the limit of detection was between approximately  $5 \times 10^5$  and  $4 \times 10^6$  molecules  $cm^{-3}$  ( $S/N = 1$ , 10 min integration) depending on the inlet configuration, flow rate, and pressure inside the FAGE detection cell, with the lowest value corresponding to the shortest inlet and lowest pressure and the

highest value corresponding to the longest inlet and highest pressure.

## 2.2 Measuring the OH interference

The OH interference was measured using a chemical titration scheme in which perfluoropropylene ( $C_3F_6$ , 99.5 %, Matheson) was added through a circular ring surrounding the detection inlet to chemically remove external OH (Griffith et al., 2016; Fig. 2). Measurements of OH concentrations using spectral modulation compared to chemical modulation with  $C_3F_6$  added externally can reveal OH radicals that are generated inside the detection cell.  $C_3F_6$  was used because it reacts quickly with OH while also having a negligible optical absorption around 308 nm (Mao et al., 2012). The injector is approximately 3.5 cm in diameter and 1.0 cm in height and consists of 10 equally spaced 0.4 mm holes in the ring that surround the inlet nozzle at the center of the injector. The holes are approximately 0.5 cm above the level of the detection cell inlet. Increasing the height of the injector above the inlet from 0.5 cm to 4.5 does not impact the overall sensitivity of the instrument, suggesting that OH radicals are not lost on the outer walls of the injector.

To determine the flow of  $C_3F_6$  to be used, OH was produced from the photolysis of ambient air using a mercury pen lamp placed in front of the inlet (Fig. S2). Once a constant OH signal was established,  $C_3F_6$  was added at varying flows to determine the flow that depleted  $\geq 90\%$  of the external OH signal (a total flow of 99.5 %  $C_3F_6$  of approximately 3–5 sccm). With the flow entering the detection cell inlet of 3–9 SLPM depending on inlet diameter size, this flow of  $C_3F_6$  results in an approximate concentration of  $1\text{--}3 \times 10^{16}$  molecules  $\text{cm}^{-3}$  and a residence time of approximately 0.05 s. This flow rate was able to titrate the externally generated OH regardless of the flow rate set by each individual inlet diameter. To ensure that this flow of  $C_3F_6$  did not titrate OH radicals produced inside the detection cell, a pen lamp was placed inside the detection cell directly behind the inlet to generate OH radicals internally. The same external  $C_3F_6$  flow was again introduced to ensure that the concentration of  $C_3F_6$  after expansion into the detection cell was not high enough to titrate any internally generated OH.

By applying this  $C_3F_6$  titration method to the alkene ozonolysis experiments, any OH produced in the flow tube was expected to be removed. Although the ozonolysis reactions may still lead to additional OH production during the residence time in the injector, kinetic simulations suggest that under the conditions of these experiments the steady-state concentration of OH in the presence of  $C_3F_6$  would be near or below the detection limit of the instrument (less than  $5 \times 10^5$  molecules  $\text{cm}^{-3}$ ). However, for some of the high concentration experiments, the amount of  $C_3F_6$  added may not have been sufficient to reduce the steady-state concentration of OH to below the detection limit of the instrument, especially for the ocimene experiments due to the high re-

activity of ocimene with ozone. However, the model simulations suggest that even for these high concentration experiments the remaining steady-state OH concentrations represented less than 10 % of the observed interference. Thus, the majority of OH that was measured using spectral modulation after  $C_3F_6$  addition would be an interference generated internally. Subtraction of this interference from the measurement acquired before  $C_3F_6$  addition should reflect the steady-state OH concentration generated in the flow tube, which can then be compared to literature values of the OH yield for the ozonolysis of these alkenes.

## 3 Results and discussion

### 3.1 Ozonolysis experiments

The interference tests were performed during the alkene ozonolysis experiments with a reaction time in the flow tube of approximately 420 ms, which is a reaction time longer than that required for the system to reach steady state (less than approximately 20 ms based on model calculations), and the results are shown in Figs. 3 and 4. In these figures, the open symbols are the measured OH concentration produced from the ozonolysis reaction without addition of  $C_3F_6$  (with interference), and the filled symbols represent the OH signal after the signal measured with  $C_3F_6$  addition is removed (without interference) using the 0.6 mm nozzle, shown on the same plot to illustrate the magnitude of the interference. The expected steady-state OH concentrations based on previous measurements of the OH yield for each compound are also shown in each figure by the solid line, calculated using the following equation:

$$[\text{OH}]_{\text{ss}} = \frac{k_{\text{O}_3+\text{VOC}}\alpha [\text{O}_3][\text{alkene}]}{k_{\text{OH}+\text{VOC}}[\text{alkene}] + k_{\text{OH}+\text{O}_3}[\text{O}_3] + k_{\text{wall}}} \approx \frac{k_{\text{O}_3+\text{VOC}}\alpha [\text{O}_3]}{k_{\text{OH}+\text{VOC}}} \quad (1)$$

In this equation,  $k_{\text{O}_3+\text{VOC}}$  is the rate constant for the  $\text{O}_3$ +alkene reaction with an OH yield of  $\alpha$ ,  $k_{\text{OH}+\text{VOC}}$  is the rate constant for the OH + alkene reaction,  $k_{\text{OH}+\text{O}_3}$  is the rate constant for the OH +  $\text{O}_3$  reaction, and  $k_{\text{wall}}$  is the first-order loss of OH on the walls of the reactor, measured as described in Hansen et al. (2014). Determining the expected steady-state OH concentration from this equation has the advantage of being independent of the concentration of each BVOC. Rate constants for the OH and  $\text{O}_3$  reactions were obtained from recommendations by Atkinson (1997) and Atkinson et al. (2006). For these calculations, the loss of OH from reaction with ozone (approximately  $7 \text{ s}^{-1}$ ) and wall loss of OH (approximately  $3.6 \text{ s}^{-1}$ ) were neglected, as they were much smaller than the loss of OH due to reaction with the alkenes due to the high concentration of alkenes used in these experiments.

As illustrated in Fig. 3, the measured OH concentration from the ozonolysis of  $\alpha$ -pinene without  $C_3F_6$  addition is consistently greater than the measurements after the interference is subtracted, indicating that a significant concentration of OH is being produced inside the detection cell. In these figures, instabilities in the concentration of ozone produced by the ozone generator resulted in small variations in the measured ozone concentrations between measurements with and without added  $C_3F_6$ . Experiments without  $\alpha$ -pinene in which ozone alone was sampled by the detection cell showed a negligible OH signal, suggesting that the interference was related to the presence of both the alkene and ozone. The observed interference measured with the addition of  $C_3F_6$  accounted for approximately 40–60 % of the observed signal in the absence of  $C_3F_6$ . When the measured interference was subtracted from the overall signal, the resulting OH concentrations were in reasonable agreement with the OH yield expected from  $\alpha$ -pinene ozonolysis resulting in an OH yield of approximately  $0.81 \pm 0.10$ , determined from a weighted fit of the slope of the plot of the OH concentration versus ozone concentration, in good agreement with the value of  $0.76 \pm 0.11$  as reported by Chew and Atkinson (1996) and the value of  $0.91 \pm 0.23$  reported by Siese et al. (2001).

The measured interference appeared to depend on the length of the inlet, with the greatest interference observed with the longest inlet (Fig. 3), while the interference measured with the short- and medium-length inlets were comparable. Similar results were observed with the use of the 1 mm nozzle diameter (Fig. S3), with the longest inlet displaying the greatest interference. These results are similar to those observed by Fuchs et al. (2016), who found that the interference from the ozonolysis of  $\alpha$ -pinene, limonene, and isoprene also increased with the length of the inlet in their FAGE instrument. But while the inlet length appears to exhibit a trend in the OH interference, the cell pressure did not appear to significantly impact the level of the interference except at the longest inlet length. These results are in contrast to the results of Fuchs et al. (2016), who found that the interference in their instrument decreased with cell pressure, although the effect was greater with the longer inlet. The different cell pressures in these experiments were obtained by changing the pumping speed, which impacts the velocity and residence time of the airstream inside the detection cell. This suggests that increasing the reaction time for the short- and medium-length inlets does not significantly impact the interference, while increasing the reaction time for the longest inlet does increase the interference. However, at the longest inlet length, the increased reaction time likely also leads to increased collisions with the interior surfaces of the detection cell, which could also lead to increased dissociation and production of OH. Increasing the nozzle diameter decreases the flow velocity inside the detection cell, which increases the reaction time and the frequency of wall collisions using the longer inlet length. Although this also increases the loss of OH generated by the interference, it appears that the rate

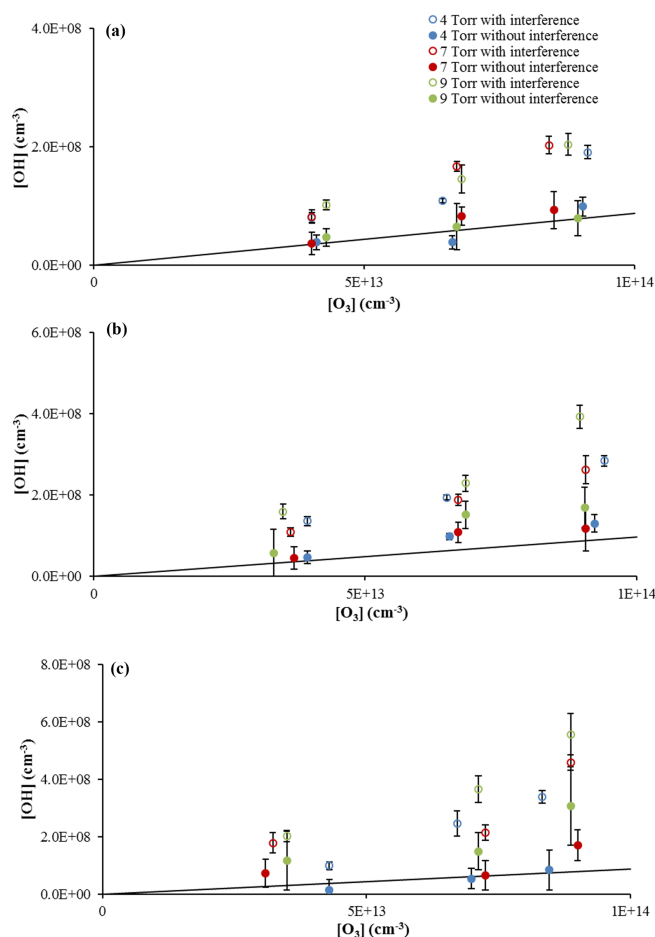


**Figure 3.** OH concentrations from  $\alpha$ -pinene ozonolysis at three cell pressures with and without the interference using the 0.6 mm diameter nozzle and the short (a), medium (b), and long (c) inlet lengths with  $\alpha$ -pinene concentrations of approximately  $3 \times 10^{12} \text{ cm}^{-3}$ . Error bars indicate the precision of the measurement ( $1\sigma$ ). Lines indicate the expected steady-state OH concentration based on published values of the OH yield (see text).

of production of OH by the interference is greater than the loss rate of OH on the walls of the inlet. These results appear to be independent of the  $\alpha$ -pinene concentration (Fig. 4a) as the level of the interference is similar for estimated  $\alpha$ -pinene concentrations between approximately  $1 \times 10^{13}$  and  $4 \times 10^{13} \text{ molecules cm}^{-3}$ .

The results from the ozonolysis of  $\beta$ -pinene are also shown in Fig. 4b. Similar to that observed for the ozonolysis of  $\alpha$ -pinene, the observed interference measured with the addition of  $C_3F_6$  accounted for approximately 40 % of the observed signal in the absence of  $C_3F_6$ . When the measured interference was subtracted from the overall signal, the measured OH concentrations results in an overall OH yield of approximately  $0.40 \pm 0.01$ , which is in good agreement with the value reported by Atkinson et al. (1992) of  $0.35 \pm 0.05$ . The percentage of interference as well as

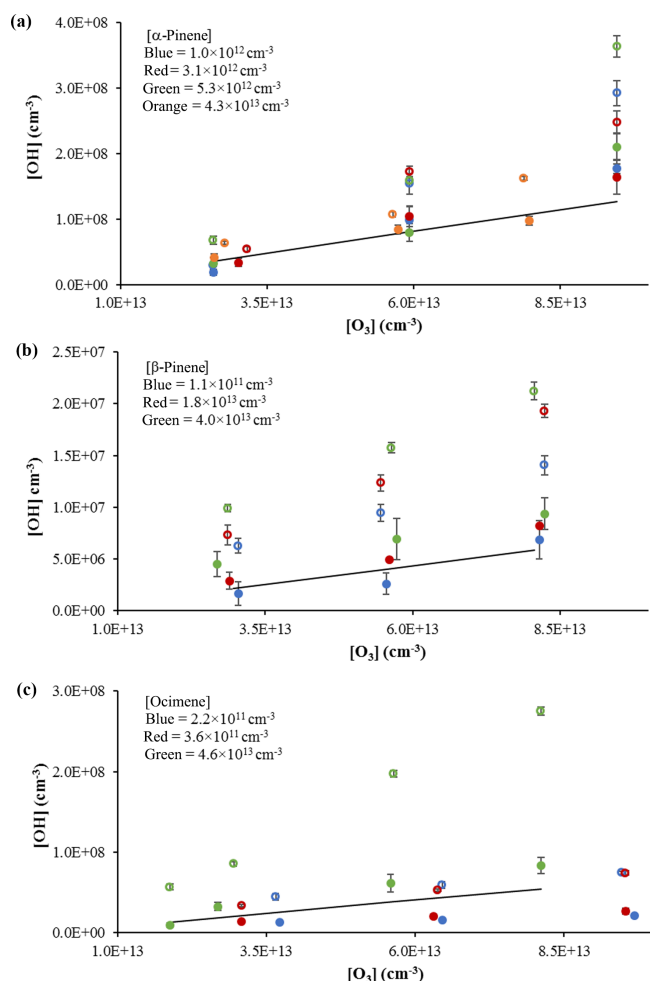


**Figure 4.** OH concentrations using the short inlet from the ozonolysis of  $\alpha$ -pinene (a),  $\beta$ -pinene (b), and ocimene (c). Open circles indicate measurements with the interference; filled circles indicate measurements without the interference. Colors indicate estimated concentrations. Solid lines reflect the expected OH radical yield (see text). Error bars reflect the measurement precision ( $1\sigma$ ).

the resulting OH yield was relatively constant for each  $\beta$ -pinene concentration used; however, the results suggest that the OH yield may increase with increasing concentrations of  $\beta$ -pinene. Measurements of the concentration of OH produced from the ozonolysis of various concentrations of ocimene are also shown in Fig. 4c. In contrast to the ozonolysis of  $\alpha$ -pinene, the interference and the observed OH yield appear to increase with increasing ocimene concentration. At ocimene concentrations of approximately  $4 \times 10^{11}$  molecules cm<sup>-3</sup>, an OH yield of approximately  $0.28 \pm 0.02$  was measured. However, the apparent OH yield increased to a yield of  $1.0 \pm 0.03$  at the highest ocimene concentration (approximately  $5 \times 10^{13}$  molecules cm<sup>-3</sup>). Additional ocimene ozonolysis experiments were performed using the two nozzle diameters and three inlet lengths with the results shown in Fig. S4. These results show that the mea-

sured OH yield from ocimene ozonolysis after subtracting the interference is only consistent with the results of Aschmann et al. (2002) of  $0.55 \pm 0.09$  for an ocimene concentration of approximately  $1 \times 10^{13}$  molecules cm<sup>-3</sup>. The increase in the apparent OH yield and interference as the concentration of ocimene was increased may be due to the additional ozonolysis of the reaction products, as the products of ocimene ozonolysis are unsaturated. The higher ocimene concentrations would lead to increased concentrations of reaction products, which in turn could also contribute to the measured interference and OH yield. Additional experiments are needed in order to better quantify the OH yield from the ozonolysis of ocimene.

In contrast to the measurements involving  $\alpha$ -pinene,  $\beta$ -pinene, and ocimene, similar ozonolysis experiments involving isoprene and MBO did not produce a detectable OH signal or interference under the highest ozone and alkene concentrations. These results may reflect the lower relative reactivity of isoprene and MBO with O<sub>3</sub> compared to reaction with OH as well as a lower yield of OH under the conditions of these experiments. Simulations of the kinetics using the Master Chemical Mechanism (MCM) for the ozonolysis of isoprene result in steady-state OH concentrations that are a factor of 50 lower than that predicted for the ozonolysis of  $\alpha$ -pinene, consistent with a lower steady-state OH concentration estimated using Eq. (1), and are near or below the detection limit of the instrument. However, these results do not rule out the possibility of an interference from the ozonolysis of these compounds. The lower reactivity of isoprene and MBO with ozone would likely require longer reaction times or higher concentrations of ozone and/or alkenes to establish steady-state OH concentrations above the detection limit of the instrument in these experiments. Fuchs et al. (2016) did find a significant unexpected OH signal in laboratory under very high concentrations of isoprene and a reaction time on the order of 1 s. Future experiments will involve higher concentrations of ozone, isoprene, and MBO and/or longer reaction times to increase the ozonolysis rate for these reactions and to determine the potential magnitude of the interference from isoprene and MBO in the IU-FAGE instrument.

### 3.2 Interference measurements as a function of laser power, ozone, and ozonolysis reaction time

A potential interference with the detection of OH radicals by laser-induced fluorescence is the production of OH through photolysis of ozone by the laser, with the resulting excited oxygen atoms reacting with ambient water vapor to produce OH (Reactions R1 and R2; Stevens et al., 1994; Ren et al., 2004):



The resulting OH signal from this two-photon process would display a quadratic dependence on laser power. One possible

source of the interference observed in the ozonolysis experiments could be  $O(^1D)$  produced from the photolysis of ozone by the laser reacting with the alkene leading to the production of OH radicals through a hydrogen abstraction mechanism. The OH signal from this two-photon process would also display a quadratic dependence on laser power.

To confirm that laser-generated OH was not occurring within this instrument and was not the source of the interference, experiments were conducted over a wide range of laser powers (0.6–12 mW) to determine whether the observed interference displayed a dependence on laser power consistent with a laser-generated mechanism. Figure 5a shows the measurements of the OH concentration with and without the interference for the ozonolysis of ocimene as a function of laser power. These experiments were done under dry conditions to minimize potential laser-generated interferences from Reactions (R1) and (R2). Because the OH concentration remained relatively stable over the range of laser powers used in these experiments, there is no indication that the interference was due to a laser-generated mechanism. These results are similar to that found by Novelli et al. (2014a) and Fuchs et al. (2016).

A plot of the interference at different ozone concentrations is also shown in Fig. 5b for the ozonolysis of  $\alpha$ -pinene as an example. Comparing the measured interference for each inlet length and ozone concentration shows a trend in which the interference appears to increase with increasing ozone concentration, with the greatest increase occurring with the longest inlet. Similar to the results of Fuchs et al. (2016), the observed interference appears to increase with the overall ozonolysis turnover time, defined as the steady-state rate of OH radical propagation, expressed here as the rate of alkene ozonolysis (Fig. 6). Although the magnitude of the interference observed here is greater due to the greater turnover rates used in these experiments, the slope of the observed interference using the short inlet as a function of the turnover rate appears to be similar to that observed by Fuchs et al. (2016), although the results presented here are highly scattered, likely due to the large uncertainty associated with estimating the concentration of each BVOC. However, the level of the observed interference is greater than that illustrated in Fig. 6 for the measurements using the long inlet, suggesting the similarity with the results of Fuchs et al. (2016) may be fortuitous, as differences in the design of the instrument impacts the level of the interference. In contrast to the results of Fuchs et al. (2016), the level of interference as a function of the turnover rate is not similar for all of the BVOCs tested. While the observed interference as a function of turnover rate appears to be similar for the ozonolysis of  $\alpha$ -pinene and ocimene, the observed interference for the ozonolysis of  $\beta$ -pinene is significantly less. This may also be related to uncertainties associated with estimates of the concentration of  $\beta$ -pinene in the flow tube but may also suggest differences in the mechanism for the production of the interference for some BVOCs. Additional measurements of the interference for other BVOCs are needed to resolve this discrepancy.

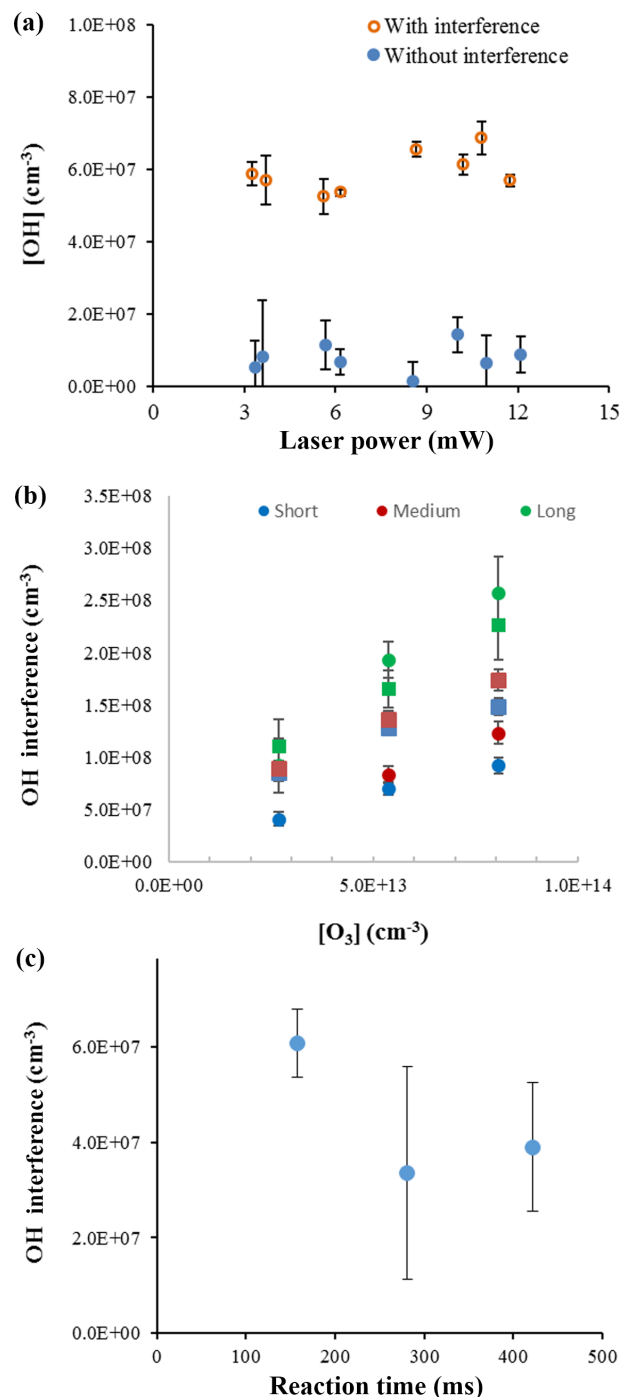


**Figure 5.** OH concentrations from ocimene ozonolysis with varied laser power at an ozone mixing ratio of 2 ppm and ocimene concentration of approximately  $3 \times 10^{13} \text{ cm}^{-3}$  (a). OH interference during  $\alpha$ -pinene (approximately  $3 \times 10^{12} \text{ cm}^{-3}$ , circles) and ocimene (approximately  $3 \times 10^{13} \text{ cm}^{-3}$ , squares) ozonolysis based on ozone concentration and inlet length (b). OH interference measurements during ocimene ozonolysis as a function of reaction time with an ocimene concentration of approximately  $3 \times 10^{13} \text{ cm}^{-3}$  (c).



The interference signals from the ozonolysis of  $\alpha$ -pinene,  $\beta$ -pinene, and ocimene for each experimental condition are summarized in Table S2. The interference from  $\alpha$ -pinene expressed as a percentage of the total OH signal at several ozone concentrations and cell pressures for the short, medium, and long inlets is shown in Fig. S5. On average, the percent interference was similar for ozone mixing ratios between 1–3 ppm, with values of approximately  $45 \pm 3$ ,  $37 \pm 8$ , and  $58 \pm 8$  % for the short, medium, and long inlets, respectively, for the 1 mm nozzle, and approximately  $54 \pm 7$ ,  $50 \pm 13$ , and  $65 \pm 11$  % for the short, medium, and long inlets, respectively, for the 0.6 mm nozzle. As discussed above, the similarity of the measured interference between the short- and medium-length inlets suggests that the level of interference is not directly related to the residence time inside the FAGE detection cell but may be the result of increased collisions with the interior surfaces of the detection cell that occurs when using the longest inlet. Similar results were observed for the ozonolysis of ocimene (Fig. S6), although additional experiments will be needed to determine whether a similar trend with inlet length and residence time is observed.

The interference was also measured over varying reaction times within the flow tube, and an example of the results is shown in Fig. 5c. The results appear to indicate that the level of interference does not depend on the ozonolysis reaction time in the flow tube. If the interference were due to a stable oxidation product, it would be expected to increase with reaction time as the concentration of stable oxidation products accumulated in the flow tube. These results suggest that the interference is not due to a stable oxidation product but may instead be due to a steady-state intermediate in the ozonolysis mechanism. The consistency of the measured interference relative to the OH concentration produced from the ozonolysis mechanism may suggest that the source of the interference is related to the source of OH, such as the Criegee intermediate.

### 3.3 Stabilized Criegee intermediates as a source of the interference

#### 3.3.1 Decomposition of Criegee intermediates produced inside the FAGE detection cell as a source of the interference

The ozonolysis of alkenes involves the addition of ozone to the double bond, forming a primary ozonide which quickly decomposes to an excited Criegee intermediate and a carbonyl compound. Depending on its structure, the excited Criegee intermediate can either decompose to form an OH radical or can be stabilized by collisions forming a stabilized Criegee intermediate, which can also thermally dissociate into OH at longer reaction times (approximately 1 s for tetramethylethylene, Kroll et al., 2001b). At shorter reaction times, the excited Criegee intermediate is in steady state with respect to dissociation and stabilization, resulting in OH con-

centrations that are generally independent of reaction time but increase at longer reaction times due to the additional OH production from SCIs (Kroll et al., 2001b). Rate constants for decomposition and stabilization of excited Criegee intermediates are estimated to be on the order of  $10^4$ – $10^9$  s<sup>-1</sup> (Horie and Moortgat, 1991), while the rate constant for decomposition of the stabilized (CH<sub>3</sub>)<sub>2</sub>COO Criegee intermediate has been measured to be on the order of  $10^2$  s<sup>-1</sup> (Smith et al., 2016). Although different Criegee intermediates will likely decompose at different rates, one might expect the concentration of excited Criegee intermediates to be very low compared to the concentration of SCIs, many of which have estimated lifetimes on the order of milliseconds relative to decomposition. The atmospheric fate of SCIs will depend on the rate of decomposition relative to reaction with other atmospheric trace gases such as SO<sub>2</sub> or H<sub>2</sub>O among others (Novelli et al., 2014b), which are also likely different for different intermediates. This lifetime may be longer in the low-pressure region of the FAGE detection cell due to the decrease in concentration of reactants such as SO<sub>2</sub> or H<sub>2</sub>O, allowing these SCIs to collide with the walls of the detection cell.

The time dependence of the observed interference in these experiments, with the interference appearing to be independent of reaction time except under the longest reaction time, at first appears to be consistent with a mechanism that involves the formation of excited Criegee radicals inside the FAGE detection cell. However, it is unlikely that excited Criegee intermediates could be produced directly from alkene ozonolysis inside the IU-FAGE detection cell as the decrease in reactant concentrations from the expansion to low pressure leads to turnover rates that are approximately 2 orders of magnitude smaller than that shown in Fig. 6. For the ozonolysis of  $\alpha$ -pinene, a reaction time of approximately 0.5–1 s would be required to internally produce the observed OH signals in these experiments, which is much longer than the reaction time inside the detection cell (on the order of 1–2 ms). The short reaction time in the detection cell is also too short for OH concentrations to reach steady state. The lower pressure in the FAGE detection cell may result in higher yields of OH due to the lower rate of stabilization of the excited Criegee intermediate under these conditions (Kroll et al., 2001a). Nevertheless, an OH yield of 1.0 would still require a reaction time of approximately 0.18 to 0.35 s to produce the observed internal OH concentrations.

#### 3.3.2 Decomposition of Criegee intermediates produced outside of the FAGE detection cell as a source of the interference

Previous measurements have demonstrated that the stabilized Criegee intermediates produced external to the FAGE detection cell from the ozonolysis of propene and (*E*)-2-butene can decompose to produce OH radicals upon entering the low-pressure region of the FAGE detection cell

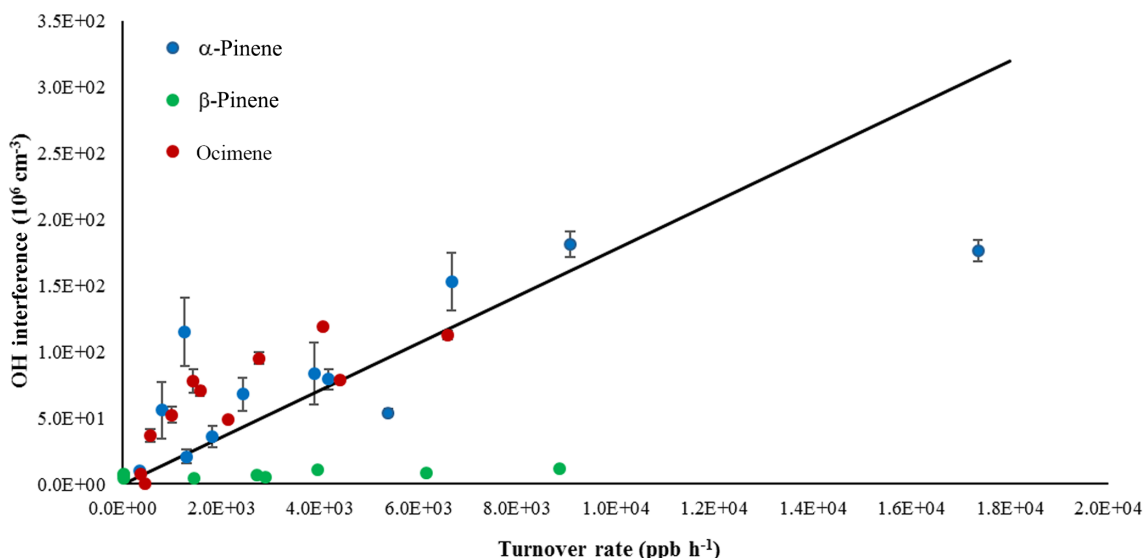


**Figure 6.** Interference signal as a function of turnover rate for the ozonolysis of  $\alpha$ -pinene,  $\beta$ -pinene, and ocimene using the short inlet. Solid line reflects the slope observed by Fuchs et al. (2016).

(Novelli et al., 2014b). The time dependence of the OH production was consistent with previous measurements of the rate of unimolecular decomposition of SCIs (Novelli et al., 2014b). To determine whether the decomposition of stabilized Criegee intermediates is the source of the interference in these experiments, acetic acid was added to the flow tube as an SCI scavenger. Welz et al. (2014) have reported direct measurements of the rate constants for the reactions of  $\text{CH}_2\text{OO}$  and  $\text{CH}_3\text{CHOO}$  Criegee intermediates with formic and acetic acids and found values in excess of  $1 \times 10^{-10} \text{ cm}^3 \text{ molecule}^{-1} \text{ s}^{-1}$ . In contrast, the rate constant for reaction of acetic acid with OH is approximately  $7 \times 10^{-13} \text{ cm}^3 \text{ molecule}^{-1} \text{ s}^{-1}$  (Atkinson et al., 2006). Acetic acid was chosen over  $\text{SO}_2$  or water as an SCI scavenger as  $\text{SO}_2$  fluorescence at 308 nm can interfere with OH measurements (Fuchs et al., 2016), while the addition of water in the presence of the high concentrations of ozone in these experiments would have led to significant laser-generated OH from Reactions (R1) and (R2). Assuming that other Criegee intermediates react similarly, addition of acetic acid should scavenge SCIs in the flow tube. If SCIs are the source of the OH interference, the measured OH signal resulting from the addition of acetic acid should be equivalent to the OH signal when the OH interference measured using external  $\text{C}_3\text{F}_6$  titration is subtracted. For these experiments, approximately  $9 \times 10^{12} \text{ molecules cm}^{-3}$  of acetic acid was introduced into the flow tube and allowed to react for approximately 200 ms. At this concentration, the reaction with acetic acid was modeled to have a minimal impact on the steady-state concentration of OH.

The results of these experiments for the ozonolysis of  $\alpha$ -pinene and ocimene are shown in Fig. 7. In this figure, the open symbols are the measured total OH signal due to OH

produced in the flow tube from both excited and stabilized Criegee intermediates plus the OH interference, while the solid red symbols represent the remaining OH signal after the interference (measured after external  $\text{C}_3\text{F}_6$  addition) is subtracted. The solid green symbols represent the measured OH signal (without external  $\text{C}_3\text{F}_6$  addition) when acetic acid is added to the flow tube. As can be seen from this figure, the measured OH signal when acetic acid is added is similar to the OH signal when the interference is subtracted, suggesting that the interference is due to the decomposition of SCIs produced from the ozonolysis of  $\alpha$ -pinene or ocimene inside the IU-FAGE detection cell, consistent with the results of Novelli et al. (2014b). These results also suggest that the majority of the OH radicals in the flow tube are produced from the rapid decomposition of excited Criegee radicals, consistent with the low yield of SCIs produced from the ozonolysis of  $\alpha$ -pinene (Drozd and Donahue, 2011). If stabilized Criegee intermediates were responsible for a significant fraction of the OH produced in the flow tube, it is likely that addition of acetic acid would have led to measured OH signals that were significantly lower than the OH signal after the interference was subtracted. However, these results do not exclude the possibility that SCIs from the ozonolysis of the other BVOCs in these experiments are also thermally decomposing and contributing to OH production in the flow tube. Recent measurements suggest that the unimolecular decomposition of the  $(\text{CH}_3)_2\text{COO}$  Criegee intermediate can be rapid and compete with the reaction of this intermediate with water or  $\text{SO}_2$  (Smith et al., 2016; Chhantyal-Pun et al., 2017). A similar rate for the decomposition of SCIs in the experiments reported here could also compete with the reaction of this intermediate with acetic acid.

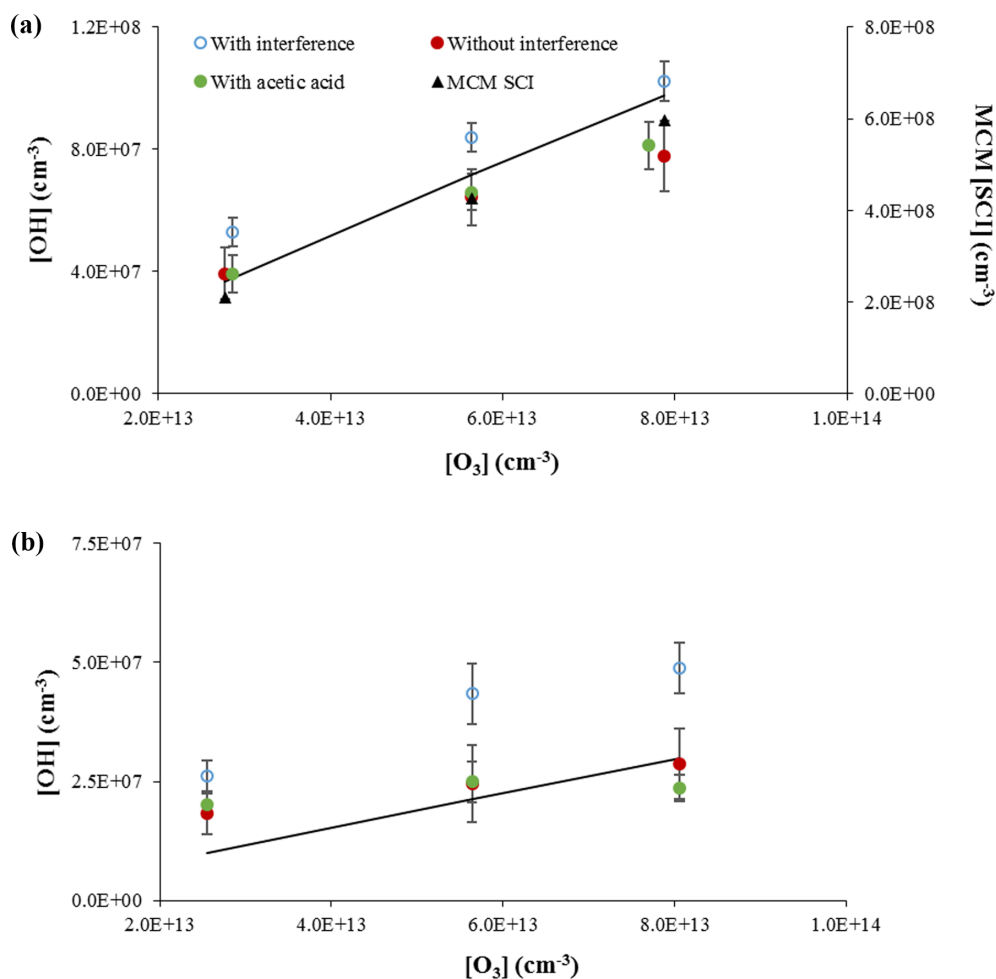


**Figure 7.** Measurements of OH concentrations from the ozonolysis of  $\alpha$ -pinene (approximately  $1 \times 10^{12} \text{ cm}^{-3}$ , **a**) and ocimene (approximately  $4 \times 10^{11} \text{ cm}^{-3}$ , **b**). Open symbols are measurements including the interference, filled red circles are the resulting OH measurements when the interference determined by  $\text{C}_3\text{F}_6$  addition is subtracted, and the filled green circles are the OH measurements when acetic acid is added to the flow tube. The lines indicate the expected OH concentration from published OH yields. The black triangles in the top plot reflect the predicted concentration of stabilized Criegee intermediates by the Master Chemical Mechanism (MCM SCI; see text).

To determine whether the magnitude of the interference observed in these experiments was consistent with the concentration of stabilized Criegee intermediates in the flow tube, the concentration of these intermediates was estimated from a chemical model of the ozonolysis of  $\alpha$ -pinene using the Master Chemical Mechanism (MCM v3.2, Jenkin et al., 1997; Saunders et al., 2003). In this mechanism, the ozonolysis of  $\alpha$ -pinene results in the formation of two Criegee intermediates, APINOOA and APINOOB. APINOOA decomposes to OH radicals through two channels with different co-products with a decomposition rate constant of  $1 \times 10^6 \text{ s}^{-1}$ . APINOOB also decomposes to form an OH radical with a decomposition rate constant of  $0.5 \times 10^6 \text{ s}^{-1}$ , but can also form a stabilized Criegee intermediate (APINBOO) with a rate constant of  $0.5 \times 10^6 \text{ s}^{-1}$ . In addition to reactions with CO, NO, NO<sub>2</sub>, and SO<sub>2</sub> (which are not significant in these experiments), the stabilized Criegee intermedi-

ate in this mechanism can also decompose to form pinonaldehyde or pinonic acid, with rate constants that depend on the concentration of water vapor ( $1.40 \times 10^{-17} \times \text{H}_2\text{O}$  and  $2.00 \times 10^{-18} \times \text{H}_2\text{O} \text{ s}^{-1}$ , respectively). This version of the MCM does not include a mechanism for the formation of OH from the stabilized Criegee intermediate, nor does it distinguish between the *syn* and *anti* isomers of the Criegee intermediates, which may have different decomposition rates and yields. Despite its potential shortcomings, the mechanism was used for simplicity to provide a rough estimate of the concentration of Criegee intermediates to compare with the experimental measurements. Given that the yield of SCIs from the ozonolysis of  $\alpha$ -pinene is relatively small (Drozd and Donahue, 2011), these shortcomings in the treatment of SCIs in the model may not significantly impact the model results.

Under the conditions of these experiments, the model predicts a steady-state concentration of stabilized Criegee intermediates (APINBOO) of approximately  $2\text{--}6 \times 10^8$  molecules  $\text{cm}^{-3}$  (Fig. 7). Based on these results, the observed OH interference in these experiments could be explained if approximately 5 % of these intermediates dissociated and produced OH radicals inside the IU-FAGE detection cell, assuming that the transmission of these stabilized Criegee intermediates through the inlet is similar to that for OH. In contrast, the MCM-predicted steady-state concentration of excited Criegee radicals (APINOOA and APINOOB) in the flow tube was calculated to be on the order of  $10^3$  molecules  $\text{cm}^{-3}$ , which is much less than the observed interference. Thus, it is unlikely that excited Criegee intermediates are the source of the interference, but rather the interference is the result of decomposition of SCIs in the FAGE detection cell. These results are in contrast to the results of Fuchs et al. (2016), who found that in their ozonolysis experiments that the addition of  $\text{SO}_2$  as a scavenger for Criegee intermediates did not affect the observed OH signal. They concluded that SCIs were not the cause of the interference in their instrument, although they could not rule out that the interference was due to the decomposition of particular SCI isomers that did not react with  $\text{SO}_2$  (Fuchs et al., 2016).

If stabilized Criegee intermediates are the source of the interference in these measurements, one might have expected to observe an interference associated with the ozonolysis of isoprene even though the expected yield of OH was below the detection limit of the instrument. Simulations using the Master Chemical Mechanism suggest that the concentration of SCIs in the isoprene ozonolysis mechanism is similar to the concentration of SCIs in the  $\alpha$ -pinene ozonolysis mechanism. Given that OH yield from the decomposition of excited CIs in the isoprene mechanism is lower than that for the  $\alpha$ -pinene mechanism, the absence of a detectable interference in the isoprene experiments described here may suggest that the decomposition of these intermediates inside the FAGE detection cell may also result in a lower OH yield. These results are also consistent with the recent study by Nguyen et al. (2016), who found that the majority of SCIs produced in the ozonolysis of isoprene were the simplest SCI,  $\text{CH}_2\text{OO}$ . The unimolecular reactivity of  $\text{CH}_2\text{OO}$  is greatly reduced compared to other SCIs due to the fact that it is non-*syn*, without any facing hydrocarbon groups (Nguyen et al., 2016), and does not lead to OH formation. Consistent with the observation that the observed interference appears to be a constant fraction of the total OH yield in these experiments independent of the ozone concentration and the turnover rate (Figs. S5 and S6), the observed interference for each alkene is likely proportional to the OH yield from the ozonolysis mechanism, with the absence of an observed interference in the isoprene experiments consistent with the lower OH yield in the isoprene ozonolysis mechanism. Additional ex-

periments measuring the interference from the ozonolysis of isoprene are needed to resolve this issue.

### 3.3.3 Interference from Criegee intermediate decomposition on LIF-FAGE calibrations

These results also imply that using the ozonolysis of alkenes as a potential source for calibrating LIF-FAGE instruments may lead to an overestimation of the instrument sensitivity given the potential for this source to produce an interference. As mentioned above, Hard et al. (2002) observed an interference in their LIF-FAGE instrument during calibrations using the ozonolysis of trans-2-butene under high mixing ratios of both ozone (up to 28 ppm) and trans-2-butene (greater than 12 ppb). They found that the interference disappeared in the presence of 1 % water vapor. Given the potentially rapid reaction of Criegee intermediates with water vapor (Chao et al., 2015), this may suggest that the source of their interference was also the decomposition of Criegee intermediates inside their detection cell. However, Dusanter et al. (2008) found that the instrument sensitivities derived from the ozone–alkene calibration technique using trans-2-butene were systematically lower than those derived from the water-vapor UV-photolysis technique, in contrast to what might be expected if the measurements from the ozonolysis technique were impacted by an interference from Criegee intermediates. But because these ozonolysis experiments were done under humid conditions, it is possible that the Criegee intermediates were scavenged by water vapor prior to entering the IU-FAGE detection cell, thus minimizing the interference. Although the rate constant of Criegee intermediates with water vapor depends on the structure of the intermediate (Vereecken et al., 2015), future calibrations of LIF-FAGE instruments using the ozonolysis of alkenes should be done in the presence of water vapor or another Criegee scavenger to ensure that the calibration is not influenced by this potential interference.

## 4 Atmospheric implications

The percent interference observed in these studies (Figs. S5, S6) is similar to the ambient measurements reported by Mao et al. (2012), who measured an interference that was approximately 50 % of the total OH signal in an environment dominated by 2-methyl-3-buten-2-ol (MBO), monoterpenes, sesquiterpenes, and related oxygenated compounds. Novelli et al. (2014a) also found that in their measurements of OH in several forest environments the interference accounted for 30–80 % of their total OH signal during the daytime. External addition of  $\text{SO}_2$  as an SCI scavenger during some of these measurements resulted in the complete removal of the interference, suggesting that the source of the interference was the decomposition of ambient SCIs inside their detection cell (Novelli et al., 2017). However, the magnitude

of the interference signal relative to the calibration for OH was much greater than the expected concentration of SCIs in these environments, which was estimated to be on the order of  $5 \times 10^4$  molecules  $\text{cm}^{-3}$  (Novelli et al., 2017). One possible reason for this discrepancy is a greater sensitivity of the LIF-FAGE instrument to the detection of ambient SCIs relative to ambient OH, perhaps due to a greater transmission efficiency of SCIs into the FAGE detection cell. Tests to measure the sensitivity of their LIF-FAGE instrument to the detection of SCIs relative to OH found that the transmission of *syn*-CH<sub>3</sub>CHOO through different nozzle designs was different from the transmission of OH radicals (Novelli et al., 2017). These results suggest that the sensitivity of their LIF-FAGE instrument may be different for the detection of SCIs and that using the calibration factor for OH radicals to estimate the SCI concentration from the interference may not be appropriate. However, the sensitivity of their LIF-FAGE instrument to detection of SCIs would have to be a factor of 100 greater than that for OH based on the estimated concentration of ambient SCIs (Novelli et al., 2017). Previous measurements on a similar LIF-FAGE instrument demonstrated that the measured OH signal is relatively insensitive to the shape and coating of the inlet (Stevens et al., 1994). In addition, external calibrations including inlet losses were found to be similar to internal calibrations that did not use the inlet. These results imply that heterogeneous loss of OH radicals on the inlet is not occurring to a significant extent (Stevens et al., 1994).

Similar to that observed by Fuchs et al. (2016), extrapolating the interference observed in the experiments presented here as a function of the ozonolysis turnover time (Fig. 6) to concentrations and turnover rates typically observed in the atmosphere (approximately  $1.5 \text{ ppb h}^{-1}$ , Hakola et al., 2012; Fuchs et al., 2016) would suggest that the interference under ambient conditions would be near the detection limit of the IU-FAGE instrument (approximately  $4 \times 10^5$  molecules  $\text{cm}^{-3}$ ). Consistent with this result, previous measurements of OH radical concentrations by the IU-FAGE instrument in an urban environment during CalNex (California Research at the Nexus of Air Quality and Climate Change) using the external chemical titration technique found no evidence of an unknown interference (Griffith et al., 2016). Measurements of OH by the IU-FAGE instrument in a forested environment in northern Michigan during and after the CABINEX (Community Atmosphere–Biosphere Interactions Experiment) campaign using the external chemical titration technique also did not reveal any unknown interferences (Griffith et al., 2013). However, the measurements during CABINEX were done under relatively cool conditions and low ozone concentrations, where daytime maximum ozone mixing ratios were approximately 30 ppb on average. The relatively cool conditions suggest that mixing ratios of BVOCs may have been relatively low during this campaign, as mixing ratios of isoprene were less than 2 ppb. During CalNex, maximum daytime mixing ratios of ozone were

higher (approximately 50–60 ppb on average during the week and approximately 70–80 ppb on average on the weekends), but mixing ratios of isoprene were even lower, less than 1 ppb on average (Griffith et al., 2016), suggesting that the mixing ratio of other BVOCs may also have been lower.

In contrast, recent measurements of OH concentrations by the IU-FAGE instrument in an Indiana forest using the external chemical titration technique did reveal an interference that correlated with both temperature and ozone concentrations, similar to the results of Mao et al. (2012) (Lew et al., 2017b). Compared to the conditions during CABINEX, these measurements were done under higher daytime maximum ozone mixing ratios (approximately 40 ppb) and relatively warmer conditions, where isoprene mixing ratios greater than 4 ppb suggest higher mixing ratios of other BVOCs. The magnitude of the observed interference (on the order of  $10^6$  molecules  $\text{cm}^{-3}$ ) was similar to that observed previously by other LIF-FAGE instruments (Mao et al., 2012; Novelli et al., 2014a, 2017) and accounted for approximately 60 % of the total measured OH signal on average. The known interference from laser-generated OH varied with laser power, ambient ozone, and water concentrations but was approximately half of the total measured interference on some days, while on other days it accounted for all of the measured interference. However, similar to that observed by Novelli et al. (2017), estimates of the ambient concentration of SCIs on the order of approximately  $4\text{--}5 \times 10^4$  molecules  $\text{cm}^{-3}$  for similar environments (Percival et al., 2013; Novelli et al., 2017) suggest that the observed interference in these measurements may not be solely due to ambient SCIs unless there are other significant sources of Criegee radicals that are not accounted for in these models.

These results suggest that, although SCIs may be contributing to the observed interference, there may exist an unknown interference in these measurements that also correlates with the concentration of ozone and BVOCs, perhaps due to oxidation products of BVOCs not tested in the experiments reported here (Fuchs et al., 2016; Novelli et al., 2017). Recently, Fuchs et al. (2016) reported an interference in their LIF-FAGE instrument associated with NO<sub>3</sub> radicals, although the exact mechanism of the interference remains unknown. These results suggest that there may be other potential interferences associated with the technique in addition to the decomposition of SCIs that involve complex homogeneous and/or heterogeneous mechanisms inside the FAGE detection cell.

## 5 Summary and conclusions

Measurements of OH concentrations produced from the ozonolysis of  $\alpha$ -pinene,  $\beta$ -pinene, and ocimene revealed a potential interference associated with the Indiana University LIF-FAGE instrument. The observed interference did not appear to be laser generated and was independent of the ozonol-

ysis reaction time. The addition of acetic acid resulted in measured OH concentrations that were similar to measurements when the interference was subtracted, suggesting that the source of the interference in these experiments involved the decomposition of stabilized Criegee intermediates inside the IU-FAGE detection cell. Further measurements and modeling will be needed for a wider variety of alkenes in order to confirm these results.

The interference appeared to increase with the length of the inlet in the low-pressure region of the detection cell, suggesting that the interference depends on the reaction time in the detection cell. However, increasing the pressure in the detection cell by decreasing the flow rate did not significantly increase the observed interference except for the longest inlet. This may suggest that the increase in the observed interference with the length of the inlet may be the result of increased collisions of the stabilized Criegee intermediates inside the detection cell leading to the formation of OH rather than the result of an increase in reaction time. Additional experiments will be needed to confirm these results. To minimize this interference and other unknown interferences, future measurements of OH by the IU-FAGE instrument will test different detection cell designs to minimize any observed ambient interferences through changes in both reaction time and potential surface collisions while also maintaining the quality of the ambient OH measurement.

Regardless, future ambient measurements by the IU-FAGE instrument will incorporate the external OH titration technique to quantify these and other potential unknown interferences. Because of differences in design (geometry, cell pressure, flow, etc.) these interference measurements may not apply to other LIF-FAGE instruments. However, it is recommended that future OH measurements using the LIF-FAGE technique incorporate an external OH titration scheme or some other method to quantify potential artifacts.

*Data availability.* Data presented in this study are available from the authors upon request (pstevens@indiana.edu).

*Supplement.* The supplement related to this article is available online at: <https://doi.org/10.5194/amt-11-1-2018-supplement>.

*Competing interests.* The authors declare that they have no conflict of interest.

*Acknowledgements.* This work was supported by the National Science Foundation, grants AGS-1104880 and AGS-1440834. We would like to thank Sebastien Dusanter for helpful comments on the manuscript.

Edited by: Hendrik Fuchs

Reviewed by: two anonymous referees

## References

- Aschmann, S. M., Arey, J., and Atkinson, R.: OH radical formation from the gas-phase reactions of O<sub>3</sub> with a series of terpenes, *Atmos. Environ.*, 36, 4347–4355, 2002.
- Atkinson, R.: Gas Phase Tropospheric Chemistry of Volatile Organic Compounds: 1. Alkanes and Alkenes, *J. Phys. Chem. Ref. Data*, 26, 215–290, 1997.
- Atkinson, R., Aschmann, S. M., Arey, J., and Shorees, B.: Formation of OH Radicals in the Gas-Phase Reactions of O<sub>3</sub> with a Series of Terpenes, *J. Geophys. Res.-Atmos.*, 97, 6065–6073, 1992.
- Atkinson, R., Baulch, D. L., Cox, R. A., Crowley, J. N., Hampson, R. F., Hynes, R. G., Jenkin, M. E., Rossi, M. J., Troe, J., and IUPAC Subcommittee: Evaluated kinetic and photochemical data for atmospheric chemistry: Volume II – gas phase reactions of organic species, *Atmos. Chem. Phys.*, 6, 3625–4055, <https://doi.org/10.5194/acp-6-3625-2006>, 2006.
- Chao, W., Hsieh, J.-T., Chang, C.-H., and Lin, J. J.-M.: Direct kinetic measurement of the reaction of the simplest Criegee intermediate with water vapor, *Science*, 347, 751–754, 2015.
- Chew, A. A. and Atkinson, R.: OH radical formation yields from the gas-phase reactions of O<sub>3</sub> with alkenes and monoterpenes, *J. Geophys. Res.-Atmos.*, 101, 28649–28653, 1996.
- Chhantyal-Pun, R., Welz, O., Savee, J. D., Eskola, A. J., Lee, E. P. F., Blacker, L., Hill, H. R., Ashcroft, M., Khan, M. A. H., Lloyd-Jones, G. C., Evans, L., Rotavera, B., Huang, H., Osborn, D. L., Mok, D. K. W., Dyke, J. M., Shallcross, D. E., Percival, C. J., Orr-Ewing, A. J., and Taatjes, C. A.: Direct Measurements of Unimolecular and Bimolecular Reaction Kinetics of the Criegee Intermediate (CH<sub>3</sub>)<sub>2</sub>COO, *J. Phys. Chem. A*, 121, 4–15, 2017.
- Drozd, G. T. and Donahue, N. M.: Pressure Dependence of Stabilized Criegee Intermediate Formation from a Sequence of Alkenes, *J. Phys. Chem. A*, 115, 4381–4387, 2011.
- Dusanter, S., Vimal, D., and Stevens, P. S.: Technical note: Measuring tropospheric OH and HO<sub>2</sub> by laser-induced fluorescence at low pressure. A comparison of calibration techniques, *Atmos. Chem. Phys.*, 8, 321–340, <https://doi.org/10.5194/acp-8-321-2008>, 2008.
- Dusanter, S., Vimal, D., Stevens, P. S., Volkamer, R., Molina, L. T., Baker, A., Meinardi, S., Blake, D., Sheehy, P., Merten, A., Zhang, R., Zheng, J., Fortner, E. C., Junkermann, W., Dubey, M., Rahn, T., Eichinger, B., Lewandowski, P., Prueger, J., and Holder, H.: Measurements of OH and HO<sub>2</sub> concentrations during the MCMA-2006 field campaign – Part 2: Model comparison and radical budget, *Atmos. Chem. Phys.*, 9, 6655–6675, <https://doi.org/10.5194/acp-9-6655-2009>, 2009.
- Faloona, I., Tan, D., Brune, W., Hurst, J., Barket, D., Couch, T. L., Shepson, P., Apel, E., Riemer, D., Thornberry, T., Carroll, M. A., Sillman, S., Keeler, G. J., Sagady, J., Hooper, D., and Paterson, K.: Nighttime observations of anomalously high levels of hydroxyl radicals above a deciduous forest canopy, *J. Geophys. Res.-Atmos.*, 106, 24315–24333, 2001.
- Fang, Y., Liu, F., Klippenstein, S. J., and Lester, M. I.: Direct observation of unimolecular decay of CH<sub>3</sub>CH<sub>2</sub>CHOO Criegee intermediates to OH radical products, *J. Chem. Phys.*, 145, 044312, <https://doi.org/10.1063/1.4958992>, 2016.
- Fuchs, H., Tan, Z., Hofzumahaus, A., Broch, S., Dorn, H.-P., Holland, F., Künstler, C., Gomm, S., Rohrer, F., Schrade, S., Tillmann, R., and Wahner, A.: Investigation of potential interferences in the detection of atmospheric ROx radicals by laser-

- induced fluorescence under dark conditions, *Atmos. Meas. Tech.*, 9, 1431–1447, <https://doi.org/10.5194/amt-9-1431-2016>, 2016.
- Guenther, A., Zimmerman, P., and Wildermuth, M.: Natural Volatile Organic Compound Emission Rate Estimates for U.S. Woodland Landscapes, *Atmos. Environ.*, 28, 1197–1210, 1994.
- Griffith, S. M., Hansen, R. F., Dusanter, S., Stevens, P. S., Alaghmand, M., Bertman, S. B., Carroll, M. A., Erickson, M., Galloway, M., Grossberg, N., Hottle, J., Hou, J., Jobson, B. T., Kamrath, A., Keutsch, F. N., Lefer, B. L., Mielke, L. H., O'Brien, A., Shepson, P. B., Thurlow, M., Wallace, W., Zhang, N., and Zhou, X. L.: OH and HO<sub>2</sub> radical chemistry during PROPHET 2008 and CABINEX 2009 – Part 1: Measurements and model comparison, *Atmos. Chem. Phys.*, 13, 5403–5423, <https://doi.org/10.5194/acp-13-5403-2013>, 2013.
- Griffith, S. M., Hansen, R. F., Dusanter, S., Michoud, V., Gilman, J. B., Kuster, W. C., Veres, P. R., Graus, M., de Gouw, J. A., Roberts, J., Young, C., Washenfelder, R., Brown, S. S., Thalman, R., Waxman, E., Volkamer, R., Tsai, C., Stutz, J., Flynn, J. H., Grossberg, N., Lefer, B., Alvarez, S. L., Rappenglueck, B., Mielke, L. H., Osthoff, H. D., and Stevens, P. S.: Measurements of hydroxyl and hydroperoxy radicals during CalNex-LA: Model comparisons and radical budgets, *J. Geophys. Res.-Atmos.*, 121, 4211–4232, 2016.
- Hakola, H., Hellén, H., Hemmilä, M., Rinne, J., and Kulmala, M.: In situ measurements of volatile organic compounds in a boreal forest, *Atmos. Chem. Phys.*, 12, 11665–11678, <https://doi.org/10.5194/acp-12-11665-2012>, 2012.
- Hansen, R. F., Griffith, S. M., Dusanter, S., Rickly, P. S., Stevens, P. S., Bertman, S. B., Carroll, M. A., Erickson, M. H., Flynn, J. H., Grossberg, N., Jobson, B. T., Lefer, B. L., and Wallace, H. W.: Measurements of total hydroxyl radical reactivity during CABINEX 2009 – Part 1: field measurements, *Atmos. Chem. Phys.*, 14, 2923–2937, <https://doi.org/10.5194/acp-14-2923-2014>, 2014.
- Hard, T. M., George, L. A., and O'Brien, R. J.: An Absolute Calibration for Gas-Phase Hydroxyl Measurements, *Environ. Sci. Technol.*, 36, 1783–1790, 2002.
- Harley, P., Fridd-Stroud, V., Greenberg, J., Guenther, A., and Vasconcellos, P.: Emission of 2-methyl-3-buten-2-ol by pines: A potentially large natural source of reactive carbon to the atmosphere, *J. Geophys. Res.*, 103, 25479–25486, 1998.
- Heard, D. E. and Pillings, M. J.: Measurement of OH and HO<sub>2</sub> in the Troposphere, *Chem. Rev.*, 103, 5163–5198, 2003.
- Hofzumahaus, A., Rohrer, F., Lu, K., Bohn, B., Brauers, T., Chang, C.-C., Fuchs, H., Holland, F., Kita, K., Kondo, Y., Li, X., Lou, S., Shao, M., Zeng, L., Wahner, A., and Zhang, Y.: Amplified Trace Gas Removal in the Troposphere, *Science*, 324, 1702–1704, 2009.
- Horie, O. and Moortgat, G. K.: Decomposition pathways of the excited Criegee intermediates in the ozonolysis of simple alkenes, *Atmos. Environ.*, 25A, 1881–1896, 1991.
- Jenkin, M. E., Saunders, S. M., and Pilling, M. J.: The tropospheric degradation of volatile organic compounds: a protocol for mechanism development, *Atmos. Environ.*, 31, 81–104, 1997.
- Kidwell, N. M., Li, H., Wang, X., Bowman, J. M., and Lester, M. I.: Unimolecular dissociation dynamics of vibrationally activated CH<sub>3</sub>CHO Criegee intermediates to OH radical products, *Nat. Chem.*, 8, 509–514, 2016.
- Kroll, J. H., Clarke, J. S., Donahue, N. M., Anderson, J. G., and Demerjian, K. L.: Mechanism of HO<sub>x</sub> formation in the gas-phase ozone-alkene reaction. 1. Direct, pressure-dependent measurements of prompt OH yields, *J. Phys. Chem. A*, 105, 1554–1560, 2001a.
- Kroll, J. H., Sahay, S. R., Anderson, J. G., Demerjian, K. L., and Donahue, N. M.: Mechanism of HO<sub>x</sub> Formation in the Gas-Phase Ozone-Alkene Reaction. 2. Prompt versus Thermal Dissociation of Carbonyl Oxides to Form OH, *J. Phys. Chem. A*, 105, 4446–4445, 2001b.
- Lelieveld, J., Butler, T. M., Crowley, J. N., Dillon, T. J., Fischer, H., Ganzeveld, L., Harder, H., Lawrence, M. G., Martinez, M., Taraborrelli, D., and Williams, J.: Atmospheric oxidation capacity sustained by a tropical forest, *Nature*, 452, 737–740, 2008.
- Lew, M. M., Dusanter, S., and Stevens, P. S.: Measurement of interferences associated with the detection of the hydroperoxy radical in the atmosphere using laser-induced fluorescence, *Atmos. Meas. Tech.*, <https://doi.org/10.5194/amt-2017-198>, in press, 2017a.
- Lew, M., Rickly, P., Bottorff, B., Sklaveniti, S., Léonardis, T., Locoge, N., Dusanter, S., Kundu, S., Deming, B., Wood, E., and Stevens, P. S.: HO<sub>x</sub> Radical Chemistry in an Indiana Forest: Measurement and Model Comparison, *Atmos. Chem. Phys.*, in preparation, 2017b.
- Mao, J., Ren, X., Zhang, L., Van Duin, D. M., Cohen, R. C., Park, J.-H., Goldstein, A. H., Paulot, F., Beaver, M. R., Crouse, J. D., Wennberg, P. O., DiGangi, J. P., Henry, S. B., Keutsch, F. N., Park, C., Schade, G. W., Wolfe, G. M., Thornton, J. A., and Brune, W. H.: Insights into hydroxyl measurements and atmospheric oxidation in a California forest, *Atmos. Chem. Phys.*, 12, 8009–8020, <https://doi.org/10.5194/acp-12-8009-2012>, 2012.
- Nguyen, T. B., Tyndall, G. S., Crouse, J. D., Teng, A. P., Bates, K. H., Schwantes, R. H., Coggon, M. M., Zhang, L., Feiner, P., Müller, D. O., Skog, K. M., Rivera-Rios, J. C., Dorris, M., Olson, K. F., Koss, A., Wild, R. J., Brown, S. S., Goldstein, A. H., de Gouw, J. A., Brune, W. H., Keutsch, F. N., Seinfeld, J. H., and Wennberg, P. O.: Atmospheric fates of Criegee intermediates in the ozonolysis of isoprene, *Phys. Chem. Chem. Phys.*, 18, 10241–10254, 2016.
- Novelli, A., Hens, K., Tatum Ernest, C., Kubistin, D., Regelin, E., Elste, T., Plass-Dülmer, C., Martinez, M., Lelieveld, J., and Harder, H.: Characterisation of an inlet pre-injector laser-induced fluorescence instrument for the measurement of atmospheric hydroxyl radicals, *Atmos. Meas. Tech.*, 7, 3413–3430, <https://doi.org/10.5194/amt-7-3413-2014>, 2014a.
- Novelli, A., Vereecken, L., Lelieveld, J., and Harder, H.: Direct observation of OH formation from stabilised Criegee intermediates, *Phys. Chem. Chem. Phys.*, 16, 19941–19951, 2014b.
- Novelli, A., Hens, K., Tatum Ernest, C., Martinez, M., Nölscher, A. C., Sinha, V., Paasonen, P., Petäjä, T., Sipilä, M., Elste, T., Plass-Dülmer, C., Phillips, G. J., Kubistin, D., Williams, J., Vereecken, L., Lelieveld, J., and Harder, H.: Estimating the atmospheric concentration of Criegee intermediates and their possible interference in a FAGE-LIF instrument, *Atmos. Chem. Phys.*, 17, 7807–7826, <https://doi.org/10.5194/acp-17-7807-2017>, 2017.
- Percival, C. J., Welz, O., Eskola, A. J., Savee, J. D., Osborn, D. L., Topping, D. O., Lowe, D., Utembe, S. R., Bacak, A., McFiggans, G., Cooke, M. C., Xiao, P., Archibald, A. T., Jenkin, M. E., Derwent, R. G., Riipinen, I., Mok, D. W., Lee, E. P., Dyke,

- J. M., Taatjes, C. A., and Shallcross, D. E.: Regional and global impacts of Criegee intermediates on atmospheric sulphuric acid concentrations and first steps of aerosol formation, *Faraday Discuss.*, 165, 45–73, 2013.
- Ren, X., Olson, J. R., Crawford, J. H., Brune, W. H., Mao, J., Long, R. B., Chen, A., Chen, G., Avery, M. A., Sachse, G. W., Barrick, J. D., Diskin, Huey, L. G., Fried, A., Cohen, R. C., Heikes, B., Wennberg, P. O., Singh, H. B., Blake, D. R., and Shetter, R. E.: HO<sub>x</sub> chemistry during INTEX-A 2004: Observation, model calculation, and comparison with previous studies, *J. Geophys. Res.*, 113, D05310, <https://doi.org/10.1029/2007JD009166>, 2008.
- Ren, X. R., Harder, H., Martinez, M., Faloona, I. C., Tan, D., Leshner, R. L., Di Carlo, P. Simpas, J. B., and Brune, W. H.: Interference testing for atmospheric HO<sub>x</sub> measurements by laser-induced fluorescence, *J. Atmos. Chem.*, 47, 169–190, 2004.
- Rohrer, F., Lu, K., Hofzumahaus, A., Bohn, B., Brauers, T., Chang, C.-C., Fuchs, H., Haseler, R., Holland, F., Hu, M., Kita, K., Kondo, Y., Li, X., Lou, S., Oebel, A., Shao, M., Zeng, L., Zhu, T., Zhang, Y., and Wahner, A.: Maximum efficiency in the hydroxyl-radical-based self-cleansing of the troposphere, *Nat. Geosci.*, 7, 559–563, 2014.
- Saunders, S. M., Jenkin, M. E., Derwent, R. G., and Pilling, M. J.: Protocol for the development of the Master Chemical Mechanism, MCM v3 (Part A): tropospheric degradation of non-aromatic volatile organic compounds, *Atmos. Chem. Phys.*, 3, 161–180, <https://doi.org/10.5194/acp-3-161-2003>, 2003.
- Schlosser, E., Bohn, B., Brauers, T., Dorn, H.-P., Fuchs, H., Häseler, R., Hofzumahaus, A., Holland, F., Rohrer, F., Rupp, L. O., Siese, M., Tillmann, R., and Wahner, A.: Intercomparison of Two Hydroxyl Radical Measurement Techniques at the Atmosphere Simulation Chamber SAPHIR, *J. Atmos. Chem.*, 56, 187–205, 2007.
- Schlosser, E., Brauers, T., Dorn, H.-P., Fuchs, H., Häseler, R., Hofzumahaus, A., Holland, F., Wahner, A., Kanaya, Y., Kajii, Y., Miyamoto, K., Nishida, S., Watanabe, K., Yoshino, A., Kubistin, D., Martinez, M., Rudolf, M., Harder, H., Berresheim, H., Elste, T., Plass-Dülmer, C., Stange, G., and Schurath, U.: Technical Note: Formal blind intercomparison of OH measurements: results from the international campaign HO<sub>x</sub>Comp, *Atmos. Chem. Phys.*, 9, 7923–7948, <https://doi.org/10.5194/acp-9-7923-2009>, 2009.
- Siese, M., Becker, K. H., Brockmann, K. J., Geiger, H., Hofzumahaus, A., Holland, F., Mihelcic, D., and Wirtz, K.: Direct measurement of OH radicals from ozonolysis of selected alkenes: a EUPHORE simulation chamber study, *Environ. Sci. Technol.*, 35, 4660–4667, 2001.
- Smith, M. C., Chao, W., Takahashi, K., Boering, K. A., and Lin, J. J.-M.: Unimolecular Decomposition Rate of the Criegee Intermediate (CH<sub>3</sub>)<sub>2</sub>COO Measured Directly with UV Absorption Spectroscopy, *J. Phys. Chem. A*, 120, 4789–4798, 2016.
- Stevens, P. S., Mather, J. H., and Brune, W. H.: Measurement of tropospheric OH and HO<sub>2</sub> by laser-induced fluorescence at low pressure, *J. Geophys. Res.*, 99, 3543–3557, 1994.
- Tan, D., Faloona, I., Simpas, J. B., Brune, W., Shepson, P. B., Couch, T. L., Sumner, A. L., Carroll, M. A., Thornberry, T., Apel, E., Riemer, D., and Stockwell, W.: HO<sub>x</sub> budgets in a deciduous forest: Results from the PROPHET summer 1998 campaign, *J. Geophys. Res.-Atmos.*, 106, 24407–24427, 2001.
- Vereecken, L., Glowacki, D. R., and Pilling, M. J.: Theoretical Chemical Kinetics in Tropospheric Chemistry: Methodologies and Applications, *Chem. Rev.*, 115, 4063–4114, 2015.
- Welz, O., Eskola, A. J., Sheps, L., Rotavera, B., Savee, J. D., Scheer, A. M., Osborn, D. L., Lowe, D., Murray Booth, A., Xiao, P., Anwar H. Khan, M., Percival, C. J., Shallcross, D. E., and Taatjes, C. A.: Rate Coefficients of C1 and C2 Criegee Intermediate Reactions with Formic and Acetic Acid Near the Collision Limit: Direct Kinetics Measurements and Atmospheric Implications, *Angew. Chem. Int. Ed.*, 53, 4547–4550, 2014.
- Whalley, L. K., Edwards, P. M., Furneaux, K. L., Goddard, A., Ingham, T., Evans, M. J., Stone, D., Hopkins, J. R., Jones, C. E., Karunaharan, A., Lee, J. D., Lewis, A. C., Monks, P. S., Moller, S. J., and Heard, D. E.: Quantifying the magnitude of a missing hydroxyl radical source in a tropical rainforest, *Atmos. Chem. Phys.*, 11, 7223–7233, <https://doi.org/10.5194/acp-11-7223-2011>, 2011.